Applied Physics Letters

RESEARCH ARTICLE | APRIL 21 2021

Enhanced performance of white organic light-emitting devices based on ambipolar white organic single crystals

Qin-Cheng Zhu; Yu Liu ✉; Ming-Hui An; Ran Ding; Gao-Da Ye; Xi Gai; Hai Wang; Ming-Xu Du; Shuo-Nan Chen; Jing Feng ✉; Hong-Bo Sun

Appl. Phys. Lett. 118, 163301 (2021)
https://doi.org/10.1063/5.0045036

Applied Physics Letters ARTICLE scitation.org/journal/apl

Enhanced performance of white organic light-emitting devices based on ambipolar white organic single crystals

Cite as: Appl. Phys. Lett. **118**, 163301 (2021); doi: 10.1063/5.0045036
Submitted: 22 January 2021 · Accepted: 5 April 2021 ·
Published Online: 21 April 2021

Qin-Cheng Zhu,[1] Yu Liu,[2,a)] Ming-Hui An,[1] Ran Ding,[3] Gao-Da Ye,[1] Xi Gai,[2] Hai Wang,[1] Ming-Xu Du,[2] Shuo-Nan Chen,[2] Jing Feng,[1,a)] and Hong-Bo Sun[4]

AFFILIATIONS

[1]State Key Laboratory on Integrated Optoelectronics, College of Electronic Science and Engineering, Jilin University, 2699 Qianjin Street, Changchun 130012, China
[2]State Key Laboratory of Supramolecular Structures and Materials, College of Chemistry, Jilin University, 2699 Qianjin Street, Changchun 130012, China
[3]Department of Applied Physics, The Hong Kong Polytechnic University, Hung Hom, Hong Kong
[4]State Key Laboratory of Precision Measurement and Technology, Department of Precision Instrument, Tsinghua University, Haidian, Beijing 100084, China

[a)]**Authors to whom correspondence should be addressed:** yuliu@jlu.edu.cn and jingfeng@jlu.edu.cn

ABSTRACT

Organic single crystals are highly promising for applications in optoelectronic devices because of their higher mobility and thermal stability than amorphous thin films. Although white organic single crystals have been fabricated by the double-doped method and applied to realize white organic light-emitting devices (WOLEDs), the unbalanced carrier transport properties of the unipolar crystals severely limit the device performance. Here, ambipolar white organic single crystals are obtained by using mixed p- and n-type molecules as an ambipolar host for the red and green dopants. The white crystal with balanced carrier transport and balanced blue, green, and red emission intensity was applied to the single-crystal WOLEDs. The highest brightness of 1956 cd m^{-2} and the current efficiency of 1.31 cd A^{-1} are achieved, which are the best performance of the single-crystal WOLEDs reported to date. A high color rendering index is obtained, which varies between 82 and 87 with increasing driving current. It is expectable that this strategy would support the practical applications of organic single crystal-based OLEDs.

In recent years, the development of white organic light-emitting devices (WOLEDs) with high brightness, efficiency, and color quality has received significant attention for their applications in solid-state lighting.[1–3] For the realization of WOLEDs with a high color rendering index (CRI), a three-color strategy (red, green, and blue) is necessary.[4,5] To realize three-color WOLEDs, structures including a multilayer construction with various emission layers or co-doping of different dye materials into the host material to achieve a multi-doping structure have been used.[6] Due to the limitations of the existing technology, amorphous films including organic small molecules and polymers are preferable for the manufacturing of OLEDs.[7] However, the random orientation of molecules in amorphous films leads to increased perturbation of the energy states of the system, resulting in increased scattering of the carriers and low carrier mobility on the order of 10^{-4} only.[5] Such low carrier mobility limits the device's ultimate performance.[8]

Organic single crystals are endowed with much greater carrier mobility compared to amorphous organic films because of their highly ordered structure and minimal defects. For example, the highest hole mobility measured in an OFET (organic field-effect transistor) on the basis of single rubrene crystals reached as high as 43 cm^2 V^{-1} s^{-1}.[9] Efficient carrier injection and transport induced by the high mobility are crucial for the high performance of the light-emitting devices.[11] Hu *et al.* constructed single-crystal light-emitting field-effect transistors (OLETs) to achieve the highest brightness among OLETs reported to date by using a high mobility organic single crystal.[10] The problem of fabricating the multi-layered structure of the single-crystal OLEDs with surface emission has been solved by the template stripping

method.[12–14,24] Various growth methods have been applied to grow organic single crystals.[26–29] Among them, the doping method has been applied to single-crystal OLEDs to realize white and three primary colors.[13] Despite these advances, unbalanced carrier transport in the crystal OLEDs due to unipolar transport properties of most organic semiconductors is an obstacle for their high performance. It has been demonstrated that it is possible to control the crystal's inherent electrical properties by mixing the n-type and the p-type materials to construct an ambipolar single crystal while maintaining a single crystal structure.[15] This strategy has been applied to crystal-based blue and red OLEDs and exhibits the potential to fabricate the organic single-crystal WOLEDs with improved performance.

In this Letter, we have demonstrated the growth of ambipolar white organic single crystals for achieving high-brightness and high-efficiency single-crystal WOLEDs. The ambipolar white single crystals were obtained by mixing the p-type 1,4-bis(4-methylstyryl) benzene (BSB-Me) and n-type 2,2′-Bis[4-(trifluoromethyl)phenyl]-5,5′bithiazole (BTPB) as a host and blue emitter and then co-doped with pentacene (Pe) and tetracene (Te) acting as the red and green emitters, respectively. The white crystal with balanced carrier transport and balanced blue, green, and red emission intensity was applied to the single-crystal WOLEDs. Our obtained WOLEDs show the highest brightness and efficiency observed for crystal WOLEDs to date, reaching 1956 cd m^{-2} and 1.31 cd A^{-1}. Meanwhile, the crystal WOLEDs show a high and stable CRI, which is varied between 82 and 87 with increasing driving current.

For pure BSB-Me (Sigma-Aldrich, Japan) crystals, a large difference between the hole mobility with the electron mobility along the *c-axis* by the time-of-flight (TOF) technique and along the *ab-plane* by the OFET technique was observed.[13,16] BTPB (Tokyo Chemical Industry Co., Ltd., Japan) contains a terminally substituted trifluoromethyl phenyl group and an electron-accepting heterocyclic ring. This modification gives the n-type thiazole oligomer great intermolecular interactions and is expected to lead to electron-acceptor behavior. In fact, the electron mobility of BTPB is 1.83 cm^2 V^{-1} s^{-1}, which is four orders of magnitude greater than that of BSB-Me.[18] Figure S1 shows the molecule structure of BSB-Me and BTPB. It was demonstrated that the charge carrier mobility will be balanced by mixing p-type BSB-Me with 10% n-type BTPB molecules.[15] Here, the ambipolar crystals grown by mixing the p-type BSB-Me and n-type BTPB are used as the dual host, and Te and Pe are doped into the mixed BSB-Me/BTPB crystal as guest materials to realize the ambipolar white crystals. We grew organic single crystals by physical vapor transport applying a tube furnace.[19,20] The sizes and shapes of the Te and Pe molecules are similar to those of the dual host (BSB-Me, BTPB) molecules enabling the host and guest molecules to freely diffuse from the vapor to the crystal surface and integrate adjacent molecules to generate a complete layer through intermolecular interactions. The sublimation temperatures of Te, Pe, BSB-Me, and BTPB are 240, 290, 270, and 270 °C.[20] Such similar sublimation temperatures enable the incorporation of guest molecules into ambipolar host materials. Before crystal growth, the host and guest materials were simultaneously ground in a mortar for several minutes to form a uniform mixed powder to ensure the uniform sublimation of the host and guest molecules. Then, the mixed powder was put in the high-temperature zone at the temperature of 270 °C, and the molecules were sublimated and transported by highly pure argon gas for the growth of mixed crystals in the low-temperature zone at 238 °C.

We fabricated WOLEDs by an improved template stripping method.[13,14,24] The dimensions of the final devices were 200 × 300 μm^2. The characteristics of the OLED were measured in the nitrogen glovebox at room temperature. The corresponding current density-voltage characteristics, brightness, EL spectra, CRI value, and CIE coordinates of the WOLEDs were obtained using a Keithley 2400 (Keithley, USA) programable voltage-current source assisted Photo Research PR-788 spectrophotometer (Photo Research, USA) from the top of the device. According to the device measuring capabilities of PR-788, the allowed measuring luminance range is between 0.7 and 103 000 cd m^{-2}. Since the size of the metal mask used is 200 × 300 μm^2, the current efficiency can be calculated based on the ratio of brightness to the light-emitting area.

The white crystals are grown with the BSB-Me:BTPB:Pe:Te ratio of 18.2:1.8:0.78:1. The desired carrier transport balance can be ensured by using the BSB-Me:BTPB ratio of 10:1.[15,21] An unipolar white crystal without the n-type BTPB and with the BSB-Me: Pe:Te ratio of 18.2:0.78:1 was grown for comparison. Figures 1(a) and 1(b) show the photographs of the ambipolar mixed blue crystal and ambipolar white crystal, respectively. The PL peak positions of the white crystals were observed at 460, 496, 530, 574, 608, and 662 nm [Fig. 1(c)] by using a fluorescence spectrophotometer (Hitachi F-4600, Hitachi, Japan). The wide emission spectra with balanced blue, green, and red emission from the white crystals are attributed to the energy transfer from the mixed host to the Pe and Te dopants. Comparison of white crystals with the 10% BTPB (ambipolar) and without the 10% BTPB (unipolar) shows that their PL peak positions are nearly coincident with each other [Fig. 1(c)]. This is because the energies of the frontier orbitals of BSB-Me and BTPB are almost identical with the HOMO energy of

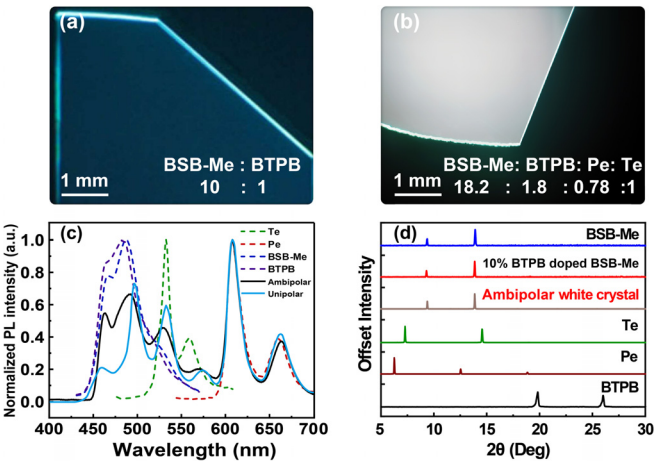

FIG. 1. Top-view photographs of the (a) ambipolar host crystal of 10% BTPB doped BSB-Me and (b) ambipolar white crystal with the BSB-Me:BTPB:Pe:Te proportions of 18.2:1.8:0.78:1 obtained under UV light irradiation using a fluorescence optical microscope. (c) PL spectra of pure Te, Pe, BSB-Me, and BTPB crystals and unipolar (BSB-Me:Pe:Te) and ambipolar (BSB-Me:BTPB:Pe:Te) white crystals. (d) Out-of-plane XRD patterns of pure BSB-Me, 10% BTPB doped BSB-Me, ambipolar white crystal, and pure Te, Pe, and BTPB.

5.6 ± 0.1 eV and the LUMO energy of 2.7 ± 0.1 eV, leading to very close energies of their emission bands.[16,18,22]

To understand the effect of the molecular doping on the molecular ordering of the white crystals, x-ray diffraction (XRD) measurements (Rigaku, D/max-rA, Japan) are performed for the pure and doped crystal in the 2θ range from 5° to 30°. As shown in Fig. 1(d), the diffraction peaks of the white crystal are consistent with those of the pure BSB-Me crystal with the peaks observed at the 2θ of 9.38° and 13.86°. The coincidence of their peak positions demonstrates that the long axis of the molecule is placed perpendicular to the crystal plane, and the ambipolar white crystal retains the ordered structure of the BSB-Me crystal. The diffraction peaks of the pure Te, Pe, or BTPB crystals are not observed in the diffraction pattern of the ambipolar white crystal, indicating that no domains of dopant molecules aggregation appear in the ambipolar white crystal. Therefore, it can be concluded that the crystal lattice framework is constructed from BSB-Me molecules, BTPB, Te, and Pe molecules, substitute some BSB-Me molecules without deformation of the crystal lattice.[23]

The carrier mobility of the ambipolar white crystal based on the mixed host material was studied by constructing top contact OFETs. The top contact OFETs are fabricated by using a 300 nm-thick SiO_2 layer and a 100 nm-thick PMMA layer together as the insulating layer of OFET, and the capacitance of the insulating layer was estimated to be 11.5 nF cm^{-2}.[25] We stick the crystal flat on PMMA through the electrostatic adsorption of tweezers. A 20 μm metal mask has been prepared as the channel of the OFET. Then, Au or Ca/Ag electrodes are deposited by vacuum thermal evaporation for effective hole and electron injection. The width of the channel is measured using a 3D depth-of-field microscope (KEYENCE, Japan). An Agilent B1500 instrument (Agilent, USA) has been used to get the output and transfer diagram of the devices. Figure 2 shows the measured charge-transport features of OFETs on the basis of ambipolar white crystals. The hole and electron mobilities are almost identical, which are $1.47 \pm 0.03 \times 10^{-3}$ cm^2 V^{-1} s^{-1} and $1.42 \pm 0.03 \times 10^{-3}$ cm^2 V^{-1} s^{-1}, respectively. To confirm that our results are repeatable, ten OFETs on the basis of ambipolar white crystals were fabricated and studied and the mobility values were obtained using ten measurements to obtain the average values and the standard deviations. On the other hand, the unipolar white crystal without the mixing of the n-type BTPB (BSB-Me:Te:Pe) shows unbalanced carrier transport characteristics with hole and electron mobilities of 4.3×10^{-3} cm^2 V^{-1} s^{-1} and 9.09×10^{-5} cm^2 V^{-1} s^{-1}.[21] The space-limited current method is also employed to directly investigate the electron mobility of the organic crystal along the *c-axis* for the ambipolar and unipolar white light crystals by fabricating an electron-only device (Fig. S2). The electron mobility of the ambipolar white crystal is two orders of magnitude higher than that of the unipolar white crystal, which is 1.1×10^{-2} cm^2 V^{-1} s^{-1} and 5.6×10^{-4} cm^2 V^{-1} s^{-1}, respectively.

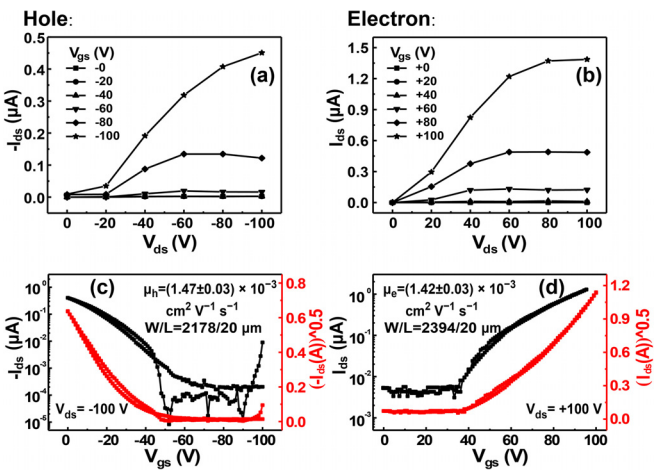

FIG. 2. (a) and (b) Output features of the OFETs on the basis of ambipolar white crystals measured in air. (c) and (d) Corresponding transfer curves of the OFETs on the basis of ambipolar white crystals measured in air. The channel width (W) and length (L) were determined by optical microscopy.

The ambipolar white crystals are applied to fabricate WOLEDs with the structure of Ag (100 nm)/MoO_3 (5 nm)/TAPC (60 nm)/ambipolar white crystal/TPBi (60 nm)/Ca (5 nm)/Ag (15 nm) [Fig. 3(a)]. Efficient carrier injection and transport can be achieved considering the HOMO and LUMO energy levels of the host molecules BSB-Me and BTPB, both of which are 5.6 eV and 2.7 eV [Fig. 3(b)].[15,21] Figure 3(b) schematically shows the graph of every layer at the relative energy level. The HOMO and LUMO energy levels of Pe are 3.2 eV and 5.0 eV, and those of Te are 2.8 eV and 5.4 eV.[17] To promote the transport and injection of carriers, MoO_3 transition metal oxide with a work function of 5.3 eV is selected as the anode modification layer and provides hole injection with gradient energy level alignment.[14] The insertion of TAPC (4,4′-cyclohexylidene bis[N,N-bis(4-methylphenyl) benzenamine]) has been proven to effectively promote the transport of holes from the anode to the crystal and improve the performance of the device.[15] TPBi has the HOMO energy of 6.1 eV and the LUMO energy of 2.8 eV and is used as an electron-transporting and hole-blocking layer.[13] The photo of the ambipolar crystal WOLEDs under working at the driving voltage of 12 V is shown in Fig. 4(a), and a bright and uniform white light emission from the WOLED surface is observed. The EL spectrum [Fig. 4(b)] shows a wide range of wavelengths with five peaks at 468, 540, 580, 608, and 664 nm covering the entire visible wavelength scope. The difference between the PL spectrum of the ambipolar white crystal and the EL spectrum of the WOLEDs can be contributed to the resonant effect of the microcavity formed by the top and bottom metallic electrodes of the WOLEDs.[24] The CRI varies from 82 to 87, and as the drive current density enhanced from 2.2 to 400 mA cm^{-2}, the CIE coordinates varied from (0.36, 0.32) to (0.35, 0.33) [the inset diagram in Fig. 4(a)].

The almost identical values of the hole and electron mobilities ensure the balanced carrier injection and transport in the emitting

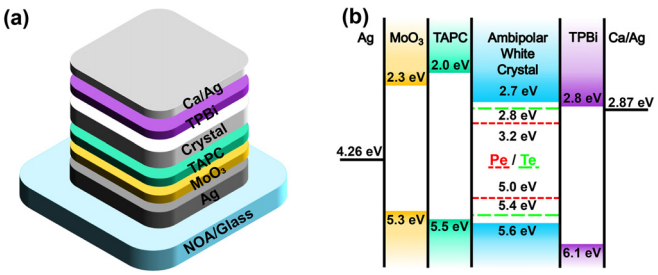

FIG. 3. (a) Device structure diagram of the ambipolar crystal WOLEDs. (b) Energy level diagram of the ambipolar WOLEDs.

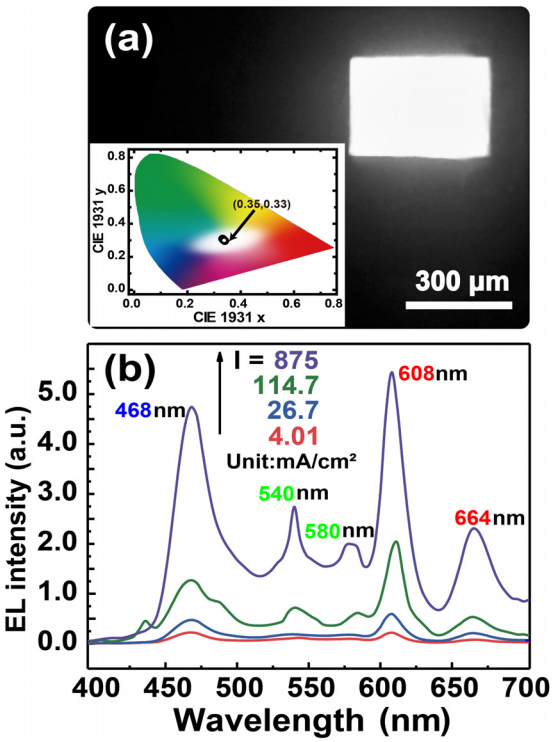

FIG. 4. (a) Photograph of operating WOLEDs based on crystals with the driving voltage of 12 V. The inset shows CIE coordinates upon the increasing current density from 2.2 to 406 mA cm^{-2}. (b) EL spectra of the WOLEDs with increased current density.

layer of the white crystal, which results in a significantly enhanced performance of the obtained WOLEDs. The current density-voltage features of the ambipolar crystal WOLEDs show that the driving voltage at the current density of 100 mA cm^{-2} is reduced from 21 V to 17 V [Fig. 5(a)]. Based on the ambipolar white crystal, we have achieved the best performance for organic single crystal WOLEDs reported to date, with a maximum brightness of 1956 cd m^{-2} that is 246% greater than that of the WOLEDs based on the unipolar white crystal [Fig. 5(a)]. The maximum efficiency is 1.31 cd A^{-1}, representing an increase of 68% relative to the efficiency of the unipolar WOLEDs of 0.78 cd A^{-1} [Fig. 5(b)]. The highest EL external quantum efficiency (EQE) is

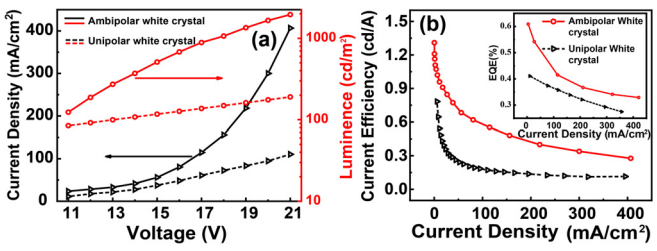

FIG. 5. EL performances of the WOLEDs on the basis of ambipolar white crystals. (a) Luminance–current density–voltage characteristics for the ambipolar WOLEDs. (b) Current density–Current Efficiency and Current density–external quantum efficiency characteristics for the ambipolar WOLEDs.

0.61%, which is 60.5% enhancement than that of the unipolar WOLEDs (0.38%) [Fig. 5(b) and Eq. (S4)]. The ambipolar white organic crystals offer great potential in high-performance WOLED applications for providing a simple structure of the single emitting layer, high CRI, and their intrinsic better thermal stability.

In conclusion, we have demonstrated almost identical hole and electron mobilities in an ambipolar white crystal prepared with a precisely adjusted proportion of ambipolar mixed host materials of BSB-Me and BTPB and by introducing Pe and Te dopants. The ambipolar white crystal significantly enhances the performance of the single crystal WOLEDs with the highest brightness and efficiency of 1956 cd cm^{-2} and 1.31 cd A^{-1}, respectively. Moreover, a high CRI is obtained from the ambipolar crystal WOLEDs, which is varied from 82 to 87 as the driving current increases. The realization of the ambipolar single-crystal WOLEDs with a multi-component mixture promotes the development of organic single crystal-based optoelectronic devices.

See the supplementary material for the structure of the BSB-Me and BTPB, measurement of the electron-only device, and the equation of the EQE.

This work was supported by the National Key Research and Development Program of China and National Natural Science Foundation of China (NSFC) under Grant Nos. 2020YFA0715000, 61825402, and 61805096.

DATA AVAILABILITY

The data that support the findings of this study are available from the corresponding author upon reasonable request.

REFERENCES

[1]Y. Huang, E. L. Hsiang, M. Y. Deng, and S. T. Wu, Light: Sci. Appl. **9**(1), 105 (2020).
[2]M. X. Yu, R. S. Huang, J. J. Guo, Z. J. Zhao, and B. Z. Tang, PhotoniX **1**(1), 11 (2020).
[3]T. Zhan, J. H. Xiong, J. Y. Zou, and S. T. Wu, PhotoniX **1**(1), 10 (2020).
[4]B. Q. Liu, M. Xu, L. Wang, H. Tao, Y. J. Su, D. Y. Gao, L. F. Lan, J. H. Zou, and J. B. Peng, Nano-Micro Lett. **6**(4), 335 (2014).
[5]D. Das, P. Gopikrishna, D. Barman, R. B. Yathirajula, and P. K. Iyer, Nano Convergence **6**(1), 31 (2019).
[6]Y. Sun, N. C. Giebink, H. Kanno, B. Ma, M. E. Thompson, and S. R. Forrest, Nature **440**(7086), 908 (2006).
[7]Y. S. Zhao, H. Fu, F. Hu, A. Peng, W. Yang, and J. Yao, Adv. Mater. **20**(1), 79 (2008).
[8]H. Nakanotani and C. Adachi, Appl. Phys. Lett. **96**(5), 053301 (2010).
[9]M. Yamagishi, J. Takeya, Y. Tominari, Y. Nakazawa, T. Kuroda, S. Ikehata, M. Uno, T. Nishikawa, and T. Kawase, Appl. Phys. Lett. **90**(18), 182117 (2007).
[10]Z. S. Qin, H. K. Gao, J. Y. Liu, K. Zhou, J. Li, Y. Y. Dang, L. Huang, H. X. Deng, X. T. Zhang, H. L. Dong, and W. P. Hu, Adv. Mater. **31**(37), 1903175 (2019).
[11]Y. Jeon, H. R. Choi, J. H. Kwon, S. Choi, K. M. Nam, K. C. Park, and K. C. Choi, Light: Sci. Appl. **8**(1), 114 (2019).
[12]R. Ding, M. H. An, J. Feng, and H. B. Sun, Laser Photonics Rev. **13**(10), 1900009 (2019).
[13]R. Ding, J. Feng, F. X. Dong, W. Zhou, Y. Liu, X. L. Zhang, X. P. Wang, H. H. Fang, B. Xu, X. B. Li, H. Y. Wang, S. Hotta, and H. B. Sun, Adv. Funct. Mater. **27**(13), 1604659 (2017).
[14]F. X. Dong, R. Ding, S. Hotta, and A. W. Li, Opt. Commun. **392**, 247 (2017).
[15]M. H. An, R. Ding, Q. C. Zhu, G. D. Ye, H. Wang, M. X. Du, S. N. Chen, Y. Liu, M. L. Xu, T. Xu, W. Wang, J. Feng, and H. B. Sun, Adv. Funct. Mater. **30**(49), 2002422 (2020).

[16]H. Nakanotani, R. Kabe, M. Yahiro, T. Takenobu, Y. Iwasa, and C. Adachi, Appl. Phys. Express **1**(9), 091801 (2008).
[17]H. Nakanotani, M. Saito, H. Nakamura, and C. Adachi, Adv. Funct. Mater. **20**(10), 1610 (2010).
[18]S. Ando, R. Murakami, J. I. Nishida, H. Tada, Y. Inoue, S. Tokito, and Y. Yamashita, J. Am. Chem. Soc. **127**(43), 14996 (2005).
[19]J. Yang, H. H. Fang, R. Ding, S. Y. Lu, Y. L. Zhang, Q. D. Chen, and H. B. Sun, J. Phys. Chem. C **115**(18), 9171 (2011).
[20]H. Wang, F. Li, B. Gao, Z. Xie, S. Liu, C. Wang, D. Hu, F. Shen, Y. Xu, H. Shang, Q. Chen, M. Yuguang, and H. Sun, Cryst. Growth Des. **9**(11), 4945 (2009).
[21]R. Ding, F. X. Dong, M. H. An, X. P. Wang, M. R. Wang, X. B. Li, J. Feng, and H. B. Sun, Adv. Funct. Mater. **29**(12), 1807606 (2019).
[22]S. Hotta, T. Yamao, S. Z. Bisri, T. Takenobu, and Y. Iwasa, J. Mater. Chem. C **2**(6), 965 (2014).
[23]R. Ding, X. P. Wang, J. Feng, X. B. Li, F. X. Dong, W. Q. Tian, J. R. Du, H. H. Fang, H. Y. Wang, T. Yamao, S. Hotta, and H. B. Sun, Adv. Mater. **30**(43), 1801078 (2018).
[24]R. Ding, J. Feng, X. L. Zhang, W. Zhou, H. H. Fang, Y. F. Liu, Q. D. Chen, H. Y. Wang, and H. B. Sun, Adv. Funct. Mater. **24**(45), 7066 (2014).
[25]Y. Zhao, X. G. Wang, M. M. Li, B. Zhang, and H. Wang, Synth. Met. **223**, 12 (2017).
[26]Z. Z. Li, F. Liang, M. P. Zhuo, Y. L. Shi, and L. S. Liao, Small **13**(19), 1604110 (2017).
[27]M. P. Zhuo, G. P. He, Y. Yuan, Y. C. Tao, G. Q. Wei, X. D. Wang, S. T. Lee, and L. S. Liao, CCS Chem. **3**(1), 413 (2021).
[28]H. Wang, Y. Zhao, Z. Q. Xie, H. Shang, H. Y. Wang, F. Li, and Y. G. Ma, CrystEngComm **17**(10), 2168 (2015).
[29]H. Wang, B. Yue, Z. Xie, B. Gao, Y. Xu, L. Liu, H. Sun, and Y. Ma, Phys. Chem. Chem. Phys. **15**(10), 3527 (2013).